Electronic structure, magnetism, and Fermi surfaces of Gd and Tb

R. Ahuja
Condensed Matter Theory Group, Department of Physics, Uppsala University, P. O. Box 530 Uppsala, Sweden

S. Auluck
Condensed Matter Theory Group, Department of Physics, Uppsala University, P. O. Box 530 Uppsala, Sweden and Department of Physics, University of Roorkee, Roorkee 247 667, India

B. Johansson
Condensed Matter Theory Group, Department of Physics, Uppsala University, P. O. Box 530 Uppsala, Sweden

M.S.S. Brooks
Commission of the European Communities, Joint Research Centre, European Institute for Transuranium Elements, Postfach 2340, W-76125 Karlsruhe, Germany

(Received 31 January 1994)

We report on local-spin-density calculations for the ferromagnetic rare-earth metals Gd and Tb using the relativistic first-principles linear-muffin-tin-orbital method in the atomic-sphere approximation. We have used a method which treats simultaneously the localized $4f$ and the conduction electron spin magnetism. The $4f$ magnetic moments are obtained from the Russel-Saunders scheme but the radial $4f$ spin density is a part of the self-consistent density-functional calculations. The calculated conduction-electron moment for Gd is in very good agreement with the measured value. The calculated de Haas–van Alphen frequencies are in agreement with available data.

I. INTRODUCTION

In the standard model for the rare-earth metals the $4f$ states are considered to be fully localized (atomic-like) and the valence electronic structure is composed of $6s$, $6p$, and $5d$ states. Although the conduction electrons make only a small contribution to the magnetic moment they play an essential role in the magnetism as the mediators of magnetic interactions. It is, therefore, important that theorists be able to calculate the conduction band electronic structure accurately. With the continuous improvement in the theories and techniques of band structure calculation, one can hope to be able to determine a variety of materials properties from first principles.[1] In this paper, we review and give details of self-consistent, relativistic, ferromagnetic calculations for gadolinium and terbium.

The first band structure calculation on gadolinium metal, reported by Dimmock and Freeman[2] using the augmented-plane-wave (APW) method, showed that the conduction electrons were primarily of $5d$ character. The calculations also showed that the Fermi surface (FS) of Gd is extremely anisotropic. Keeton and Loucks[3] reported relativistic APW calculations on Gd, Dy, Er, and Lu and found that the FS of Dy, Er, and Lu are quite similar to that of Y whereas Gd differs by the absence of a "webbing" feature. Harmon and Freeman[4] published the first spin-polarized APW calculations using a warped-muffin-tin potential and calculated conduction-electron polarization, spin densities, and neutron magnetic scattering in ferromagnetic Gd metal. They also found that the conduction-electron spin density was of mostly d character.

Harmon[5] performed the first self-consistent calculation for Gd and obtained a net conduction-electron moment which was in good agreement with the measured value. He also showed that the belly and neck orbits for the band-3 spin-up surface could be brought into agreement with experiment by a slight upward shift of the Fermi level. Sticht and Kübler[6] made self-consistent calculations for ferromagnetic Gd using the augmented-spherical-wave (ASW) method. They argued that the ground state properties of Gd could adequately be described by local spin density functional approximation (LSDA) when the $4f$ electrons are treated as part of the valence bands. A fully relativistic first-principles electronic structure calculation for magnetic materials by Krutzen and Springelkamp[7] using the ASW method showed some improvement over the scalar relativistic ASW calculations of Sticht and Kübler.[6] The calculated lower value of the magnetic moment and spectroscopic splitting factor g in comparison to the earlier ASW calculation compares well with experiment. Temmerman and Sterne[8] calculated the electronic structure of Gd in LSDA using the linear-muffin-tin-orbital (LMTO) method. They included spin-orbit coupling as well as spin polarization in their calculations and found a reasonable description of the electronic structure. In the recent work by Singh,[9] using full potential linearized augmented-plane-wave method, it was argued that a localized treatment of the $4f$ orbitals is not adequate since in the absence of f-d hybridization the small Fermi surface orbits observed experimentally could not be described. Kim *et al.*[10] have measured the temperature dependence of the exchange splitting in Gd and find good agreement with their own band structure calculation. Vescovo *et al.*[11] have performed angle resolved photoemission on Gd(0001). Recently, Sandratskii and Kübler[12] have performed calculations to study the stability of induced magnetic moments of conduction electrons in Gd with respect to disorder in the spatially localized

$4f$ moments.

The first de Haas–van Alphen (dHvA) measurement on Gd was made by Young, Jordan, and Jones[13] (YJJ). They observed four frequencies near the c axis and three frequencies in the basal plane. Later Schirber *et al.*[14] measured FS cross sections for fields along principal symmetry directions which were in serious disagreement with those of YJJ.[13] They have attributed this disagreement to an incorrect value for the saturation magnetization used by YJJ.[13] In another paper, Young, Jordan, and Jones[15] have examined the magnetoresistance of Gd and verified the multiply connected FS of minority carriers in the basal plane. Later, Mattocks and Young (MY)[16] extended the earlier dHvA measurements and observed some new small frequencies. Most of these frequencies were accounted for as occurring along Γ to K in the spin-$\downarrow$ bands. They have identified the FS as consisting of two majority surfaces and one minority surface. Using the dHvA effect Sondhelm and Young[17] have determined the cyclotron masses and mass enhancement in Gd and obtained enhancements in the range of 1.2 to 2.1 which were in agreement with the only theoretical prediction available at that time, but smaller than those suggested by low-temperature heat-capacity measurements.

Jackson[18] has calculated the electronic structure of Tb using the relativistic augmented-plane-wave (RAPW) method. He has shown that the Fermi surface of Tb consists of two surfaces: An ionic column of holes due to band 3, and surrounding this, a collection of bottles and pipes of electrons due to band 4. Further, he found that the Fermi surface is very sensitive to the Fermi energy near L as bands 3 and 4 become degenerate at L. Mattocks and Young[19] have observed only one low dHvA frequency in Tb and have interpreted this as arising from the closed band-4($\downarrow$) surface at H. The high value of the cyclotron mass for this low frequency is indicative of a large mass enhancement. More recently, Wu *et al.*[20] have measured the band structure of Tb(0001) by angle resolved photoemission and find good agreement with their own relativistic LMTO calculation.

II. METHOD OF CALCULATION AND ELECTRONIC STRUCTURE OF Gd METAL

We discern three approaches to the calculation of conduction-electron band structure in the rare earths. In the first, the $4f$ states have been treated as part of the band structure.[5] This treatment is most suitable for Gd where the seven filled spin-up $4f$ states lie self-consistently below, and the empty spin-down f states above, the Fermi energy. The splitting between these two sets of $4f$ states is easily estimated to be seven times the $4f$-$4f$ exchange integral ($J_{4f4f} \approx 0.69$ eV) or 4.8 eV. According to Singh[9] fully self-consistent calculations yield a splitting of 5 eV between up and down spin $4f$ bands, the up spin states lying about 4.5 eV below E_F and the down $4f$ bands about 0.5 eV above E_F. The spin-down $4f$ bands are quite close to the Fermi level, raise the state density at the Fermi energy through hybridization with the $5d$ states, and they increase the calculated state density at the Fermi energy to 27 states/Ry. This can be compared with a value deduced from measurements[21] and assuming no electron-phonon enhancement, of 21.35 states/Ry. The $4f$ character at the Fermi energy in Gd is, according to Singh,[9] about 5 states/Ry and it is reasonable to assume that it is responsible for the difference between theory and measurement. Precisely this problem had been detected earlier by Harmon[5] who artificially raised the $4f$ spin-down bands to remove their influence upon the state density at the Fermi energy. It is tempting to attribute the error in the position of the spin-down bands to the absence of a large Hubbard U repulsion[22] in the local spin density approximation.

The example of Gd identifies the main problem associated with leaving the $4f$ states in the band structure. The position in energy of the $4f$ bands is incorrect and the hybridization with other conduction-electron states is too large. The situation is far worse for the other lanthanide metals since in spin-polarized calculations a spin shell is not filled and the $4f$ bands, which act as a sink for electrons, always cut the Fermi level leading to specific heat coefficients which are absurdly larger than those measured.

The second approach, which is more recent, is to incorporate the self-interaction correction (SIC) in the energy band calculations.[23] SIC, as its name suggests, uses complete cancellation between the Coulomb interaction of an electron with itself and its exchange and correlation self-energy—a cancellation which is incomplete in LSDA. Inclusion of SIC results in localized states being localized further, and the energies of occupied and unoccupied states are split. Svane and Gunnarsson[24] have applied SIC to the transition metal oxides, obtaining a drastic improvement in band gaps and calculated moments compared with the results of LSDA. The most favorable aspect of SIC in its application to rare earths is the existence of separate occupied and unoccupied states. Szotek, Temmerman, and Winter[25] have applied the scheme to praseodymium metal. The occupied $4f$ states are pulled well below the conduction bands whereas the unoccupied $4f$ bands lie about 1 eV above the Fermi energy.

The third approach has been to treat the $4f$ states as part of the core as is compatible with their localized status. This not only reduces the calculated specific heat coefficients but actually makes self-consistent calculations more stable since the sensitivity of the energy of the $4f$ bands to their own occupation may easily lead to oscillations in the $4f$ occupation number. This approach has been used very successfully for the computation of cohesive properties by Skriver[26] and Eriksson *et al.*[27] Those details of the conduction bands which influenced the crystal structure were reproduced very well in Skriver's work. For example, the partial $5d$ occupation numbers decreased across the series, with a corresponding increase in the $6s$ occupation. An increase in $5d$ occupation is what causes the structural sequence hexagonal-close-packed (hcp) $\rightarrow$Sm structure $\rightarrow$ double hcp (dhcp) $\rightarrow$ fcc as the atomic number is decreased or the pressure is increased.

In this approximation the $4f$ moments, being part of

the core, cannot be computed self-consistently but the moments are known in the limit that Russel-Saunders coupling is a good approximation. The total number of $4f$ electrons is known and the spin occupation numbers are determined by applying the standard Russel-Saunders coupling scheme to the $4f$ shell. Then S is maximized, L is maximized for a given maximum S, and the total momentum $\vec{J}$ is $\vec{J} = \vec{L} + \vec{S}$. The magnetic moment is given by $\vec{\mu}_{4f} = g_J \vec{J}$ where g_J is the Landé factor. The ground state spin component of the total $4f$ moment μ^s_{4f} is obtained from the projection of the spin along the direction of total angular momentum

$$\mu^s_{4f} = 2(g_J - 1)J. \tag{1}$$

The $4f$ spin-up and spin-down occupation numbers are then determined by

$$n_{4f} = n^+_{4f} + n^-_{4f}, \quad \mu^s_{4f} = n^+_{4f} - n^-_{4f}, \tag{2}$$

where $n^{\pm}_{4f}$ are the up and down spin occupation numbers and n_f is the total number of $4f$ electrons. It is this approximation that we have tested thoroughly and report here.

We have used Andersen's LMTO method in the atomic-sphere approximation (ASA).[28,29] The calculations are self-consistent, spin polarized in the open core approximation described above, and in the Fermi surface studies spin-orbit coupling was included. Calculations for the paramagnetic ground state have been made by Lindgård[30] and Harmon.[5] The state density at the Fermi energy per atom per spin was found to be around 28 by Harmon,[5] 25 by Lindgård[30] and we calculate 22 states/Ry atom spin. Calculations with the $4f$ states polarized in the bands have been made by Harmon,[5] Sticht and Kübler,[6] Temmerman and Sterne,[8] Krutzen and Springelkamp,[7] Richter and Eschrig,[31] and Singh.[9] There seems to be general agreement that the state density at the Fermi energy is in the range 25–37 states/Ry atom spin, to which there is a $4f$ contribution of about 5–6 states/Ry atom spin. The exception was Harmon[5] who found that the state density drops to about 11 states/Ry atom spin in the polarized case. The present calculations with the $4f$ states polarized in the core or with an exchange splitting applied[32] yield a state density at the Fermi energy of 12 states/Ry atom spin. The latter calculations yield results that are on the correct side of experiment.

The calculated magnetic moments from most calculations are in good agreement with measurements[33] of $7.63\mu_B$. We obtain $7.65\mu_B$, Singh[9] obtained $7.57\mu_B$, and Temmerman and Sterne[8] $7.68\mu_B$. One difference, however, between the two types of polarized calculations is that when the $4f$ states are treated as bands the $4f$ moments turn out to be slightly less than seven, and the conduction-electron moments to be correspondingly greater. In all cases the calculated moment is within a few percent of experiment and it is reasonable to claim that the splitting of the conduction bands is approximately correct and that the LSDA exchange interactions are of about the correct strength in rare earths. We have calculated the conduction-electron moment as a function of $4f$ moment when the Gd spin is changed from 1 to 7 (Fig. 1). The conduction-electron moment is approximately (but not exactly) a linear function of $4f$ spin which indicates that a Stoner model for the conduction bands should be useful. The reason that the conduction-electron moment increases less rapidly for larger values of the $4f$ moment is that the state density at the Fermi energy starts to fall as the splitting of the conduction bands increases.

We have calculated the FS orbital areas and masses using Stark's[34] area-mass routine. The area and masses of the computed surfaces in a plane normal to a direction (i.e., the magnetic field) were found by numerical integration of the radii calculated at a fixed interval of rotation in that plane. In the calculations reported here the stepping angle $\delta\theta$ was taken to be five. Making this 2.5 changed the calculated areas by less than 0.5%. We then calculated the shift in Fermi energy ΔE_F required to bring the calculated extremal area in agreement with the experiment

$$\Delta E_F = \frac{1}{\pi} \frac{A_{\text{exp}} - A_{\text{calc}}}{m_b},$$

where m_b is the calculated mass for the orbit. The extreme ΔE_F is a measure of the error. This is meaningful since we are calculating energy eigenvalues. It would be futile to aim for an extreme ΔE_F less than the accuracy of the eigenvalues. We feel this is a better way of characterizing error than by percentages. We would like to stress that the area-mass codes calculate eigenvalues at each $\vec{k}$ point on the FS and uses no fitting procedures. There is no need for fitting as the LMTO method is very fast.

With the purpose of determining how spin-orbit coupling would influence the shape of the Fermi surface, we have first done scalar-relativistic calculations for the Fermi surface of Gd and as a second step we have included the spin-orbit coupling. To borrow from our conclusions, inclusion of spin-orbit coupling results in small changes in the calculated dHvA frequencies and band masses expect for the smaller frequencies and for orbits lying in the AHL plane. This is due to the fact that in

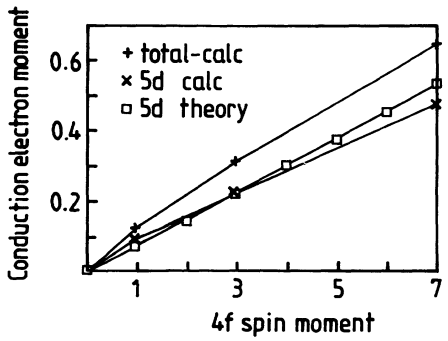

FIG. 1. The self-consistently calculated total and partial $5d$ moments per cell (two atoms) in units of Bohr magneton (μ_B) for Gd metal as a function of $4f$ spin moment (μ_B). The approximate partial $5d$ moment was obtained from Eq. (14).

Gd and Tb, the d bands are broad and this leads to a very small effect of the spin-orbit coupling.

A. Fermi surface results for gadolinium metal

The band structure along various symmetry directions is shown in Fig. 2. We only show the bands near the Fermi energy (E_F). Bands 5–7 (i.e., three bands) cross the Fermi level. The fifth and sixth band FS corresponds to spin $\downarrow$, while the seventh is spin $\uparrow$. The FS obtained from the band structure is shown in Fig. 3. The FS arising from the fifth and sixth bands is in general agreement with that obtained by using the RAPW method[5] and LMTO method[8] although in detail there are some differences. For $\vec{H}$ along [0001] the bands 5 and 6 support three extremal orbits (two central and one noncentral) each. These are obtained by calculating the area of the FS slice $A(k_H)$ centered at k_H which is the distance along the ΓA axis. The FS topology of the seventh band is different from that obtained by the other workers. We have calculated the extremal areas of all the FS sheets and our results are compiled in Table I.

We now attempt to identify our calculated areas with those measured by Mattocks and Young[16] and Schirber *et al.*[14] Some FS orbits have been identified by MY and we use their notation. Some of the measured dHvA frequencies are given in Table I. We identify the various branches as follows: The α_1 branch as arising from the fifth band in the ΓKM plane, the γ_1 branch as arising from the sixth band in the ΓKM plane, the α_2 branch is identified with the fifth band, noncentral orbit centered at a distance $\frac{2}{3}\Gamma A$ from Γ along ΓA line, and the β_1 orbit as arising from the seventh band. We have also calculated areas for the α_3 and γ_2 orbits which were measured when the magnetic field $\vec{H}$ was tilted 16% away from the [0001] axis. We agree with the assignment of MY, i.e., the α_3 orbit arises from the fifth band with the center at A and the γ_2 orbit from the sixth with the center at $\frac{2}{3}\Gamma A$ from Γ along ΓA line. Our calculated areas are in agreement with the data of MY, the worst disagreement being for the α_1 orbit. To bring the calculated area in agreement with experiment would require a shift in E_F of about 16 mRy. For the others, the shift is less than 10 mRy. If we identified α_1 as arising from fifth band with the center at A, it would require a shift in E_F of about 6 mRy.

We have also calculated some FS orbits using a converged charge density obtained by including spin-orbit coupling. The calculated frequencies for some orbits are given in Table I. Although the changes in the FS orbit areas bring them closer to experiment, the changes are, however, very small except on the AHL plane where the spin-orbit coupling has the largest effect. If we identify the α_1 orbit as arising from the fifth band with the orbit center at A then the shift in E_F required to bring the calculated area in agreement with experiment reduces to 4 mRy.

We do not find any of the small FS orbits (with frequencies less than 10^7 G) measured by MY. However a look at our band structure indicates that these could come from the seventh band (in the M-L direction) if E_F is increased by 2 mRy or from the seventh band if E_F is increased by 5 mRy. Thus one could calculate the frequencies of the small FS orbits by shifting the Fermi energy. These shifts are not uncommon and have been found in the noble metals[35] too.

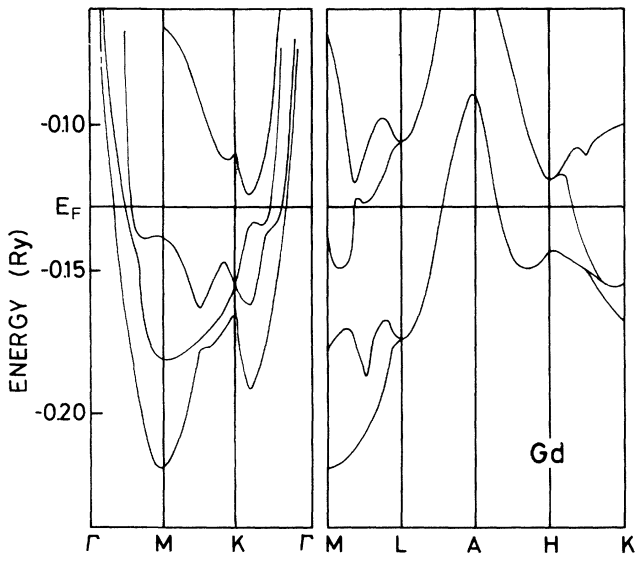

FIG. 2. Scalar-relativistic band structure of ferromagnetic Gd at the experimental lattice constant along the major symmetry directions near the Fermi level (E_F).

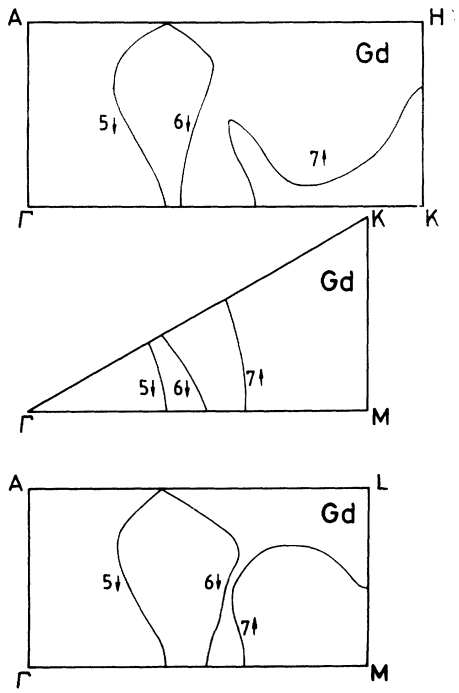

FIG. 3. Intersections of the calculated Fermi surface of Gd with the major symmetry planes. The spin up ($\uparrow$) and spin down ($\downarrow$) show the majority and minority states, respectively.

TABLE I. Calculated and experimental dHvA frequencies (in 10^7 G) and masses for Gd. The calculated dHvA frequencies, including spin-orbit coupling, are given in brackets. NC stands for noncentral orbits.

$\vec{H}$ direction	Band and orbit center	Frequency expt.[a]	Frequency[b] calc.	Mass calc.	Mass expt.[c]	MY[a] identification
(0001)	5,Γ	4.0,4.07[d]	5.47 (5.36)	-0.73	1.21	α_1
	5,NC	1.35,1.63,(1.39,1.69)[d]	2.19 (2.05)	-0.66	1.19	α_2
	5,A		5.42 (4.86)	-1.89		
	6,Γ	6.9	7.77 (7.44)	-1.71	2.2	γ_1
	6,A		5.42 (5.06)	-1.89		
	6,NC	-	11.20 (10.37)	-2.88		
	7,Γ		14.07 (14.27)	-1.55		
	7,NC		11.22	-2.53		
	5,A	2.45[e]	3.66	-1.08		α_3
	6,NC	8.7[e]	10.20	-2.25	3.2	γ_2
$(10\bar{1}0)$	7,K		3.45	1.94		
$(11\bar{2}0)$	7,M	4.5,4.66[a]	5.80 (5.51)	1.67	2.28	β_1

[a] Mattocks and Young (Ref. 16).
[b] Frequency in G×2.673 × 10^{-9} = area (in a.u.).
[c] Sondhelm and Young (Ref. 17).
[d] Schirber *et al.* (Ref. 14).
[e] 16° from [0001].

B. Fermi surface results for terbium metal

The band structure of Tb, in the vicinity of E_F, along various symmetry directions is shown in Fig. 4. Four bands (5–8) cut the Fermi level giving rise to four FS sheets. This Fermi surface is shown in Fig. 5. Bands 5 and 6 give rise to continuous noncylindrical FS sheets parallel to the ΓA line. With the magnetic field $\vec{H}$ along [0001] these support five FS orbits. Three are central with centers at Γ and A and two are noncentral with the orbit center along ΓA. The FS corresponding to the seventh band is complicated and supports extremal orbits for $\vec{H}$ along various symmetry directions. The eighth band gives rise to a closed electron FS sheet centered along the ΓK line. This small FS sheet gives rise to low dHvA frequencies. The dHvA frequencies for the various FS orbits are given in Table II.

When comparing the FS of Tb with that of Gd we see many similarities. In particular bands 5, 6, and 7 give rise

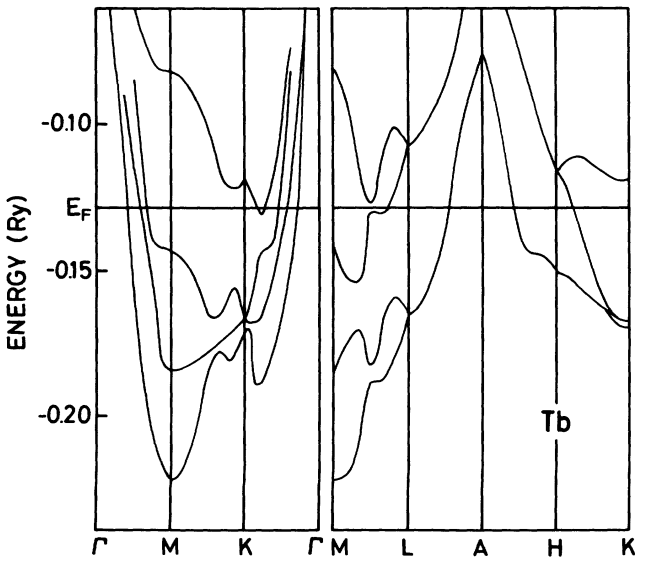

FIG. 4. Scalar-relativistic band structure of ferromagnetic Tb at the experimental lattice constant along the major symmetry directions near the Fermi level (E_F).

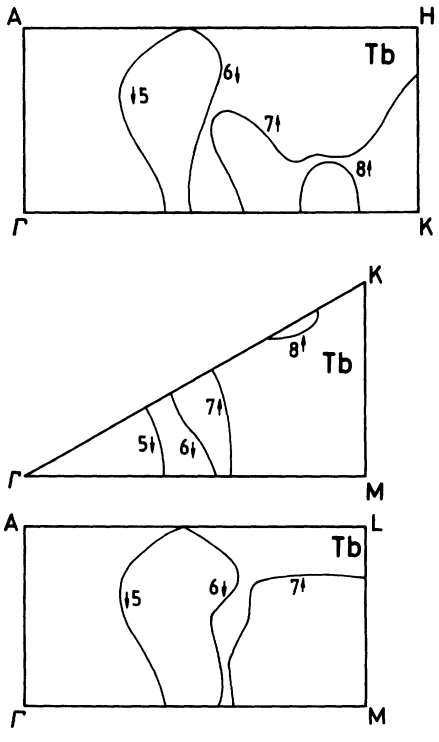

FIG. 5. Intersections of the calculated Fermi surface of Tb with the major symmetry planes. The spin up (↑) and spin down (↓) show the majority and minority states, respectively.

TABLE II. Calculated dHvA frequencies (in 10^7 Gauss) and masses for Tb. The calculated dHvA frequencies, including spin-orbit coupling, are given in brackets. NC stands for noncentral orbits.

$\vec{H}$ direction	Band and orbit center	Frequency[a]	Mass
(0001)	5,Γ	5.88 (5.79)	-0.78
	5,A	7.52 (6.88)	-2.38
	5, NC	2.66	-0.73
	6,Γ	9.20 (8.98)	-2.00
	6,A	7.52 (7.23)	-2.38
	6,NC	12.90	-3.65
	7,Γ	13.30 (13.41)	-1.48
	7,NC	11.40	-2.65
	8,ΓK	0.12 (0.077)	0.38
$(10\bar{1}0)$	7,K	5.07	2.50
	8,ΓK	0.47 (0.33)	1.07
$(11\bar{2}0)$	7,M	6.34	1.93
	8,ΓK	0.28 (0.20)	0.73

[a]Frequency (G)=area (a.u.)/2.673×10^{-9}.

to similar FS topologies. The band-8 FS appears in Tb as the bottom of the eighth band lies about 2 mRy below E_F. In Gd, however, the bottom of the eighth band lies about 5 mRy above E_F. Unlike the case of Gd, there is not sufficient data on the dHvA effect in Tb. In fact, there exists only a single measured dHvA frequency (area = 0.00195 a.u. and mass = 0.58 m_0) (Ref. 19) for $\vec{H}$ along $[10\bar{1}0]$ which was identified as arising from the H centered cap. We do not find any evidence for such a FS sheet. In our calculations the seventh to eighth band lies 13 mRy above E_F at the symmetry point H. However, we do find a small FS arising from the seventh band centered along ΓK which could explain this data. Our calculated area for this orbit is 0.0125 a.u. Using the calculated mass we obtain a shift in E_F by 3 mRy to bring the calculated area in agreement with experiment. We have calculated some FS areas including the effect of spin-orbit coupling. These are also given in Table II. Although most orbits are not affected much by spin-orbit coupling, the eighth band FS areas are changed significantly. In fact, the only measured FS area is now in better agreement with our calculations.

III. A MODEL FOR THE INFLUENCE OF THE LOCALIZED MOMENTS UPON THE BAND STRUCTURE

The conduction bands transmit the exchange interactions between the local atomic moments. We first summarize the standard model of magnetic interactions in rare earths.[36] The exchange interaction between any pair of electrons is usually written in terms of their spins as $-2J_{12}\vec{s}_1.\vec{s}_2$, where J_{12} is the interatomic exchange integral. For rare earths the exchange interaction Hamiltonian between conduction electrons and local $4f$ moments is

$$H_{s-f} = -2\sum_{4f} \tilde{J}_{4f-c} s_{4f} s_c = -2\tilde{J}_{4f-c} S_{4f} s_c$$
$$= -2\tilde{J}_{4f-c}(g_J - 1) J_{4f} s_c, \quad (3)$$

where $\tilde{J}_{4f-c}$ is an average taken over the ground state J multiplet, $\vec{J}_{4f}$ is the total $4f$ angular momentum and $\vec{s}_c$ is the conduction-electron spin. The exchange interaction is often called the s-f interaction for historical reasons[37] but it is not intended to imply here that the conduction-electron states are pure s states. In fact, in rare-earth metals and compounds the $5d$ states are more important. The s-f exchange integral is, explicitly,

$$\tilde{J}_{4f-c}(n'\vec{k}', n\vec{k}) = \int \Psi_{n'\vec{k}'}(\vec{r}) \Phi_{4f}(\vec{r}\,' - \vec{R}_i) \frac{e^2}{|\vec{r} - \vec{r}\,'|}$$
$$\times \Psi_{n\vec{k}}(\vec{r}\,') \Phi_{4f}(\vec{r} - \vec{R}_i) d\vec{r}\, d\vec{r}\,'. \quad (4)$$

The exchange integrals are always positive and they align the conduction and $4f$ spin moments to be parallel. In the ordered phase at zero temperature the rare-earth moment may be replaced by its expectation value in the mean field approximation. The s-f Hamiltonian still has both diagonal and off diagonal elements among conduction-electron states since the unperturbed states are for the paramagnetic phase. The diagonal contribution to the conduction band energies splits the spin-up and spin-down conduction bands

$$\epsilon^{\pm}_{nk} = \epsilon_{nk} \mp \langle J^z_{4f} \rangle (g - 1) \tilde{J}_{4f-c}(n\vec{k}, n\vec{k}). \quad (5)$$

In second order the energies are further modified by a contribution involving interband transitions. This second order contribution is due to the change of wave functions induced by magnetic ordering since the unperturbed wave functions are for the paramagnetic ground state, and the induced potential is nonuniform. The first order splitting of the conduction bands, Eq. (5), leads to an approximate conduction-electron moment

$$\langle \mu_z \rangle_c = \mu_B N(\epsilon_F)(g_J - 1) \langle J^z_{4f} \rangle \tilde{J}_{4f-c}, \quad (6)$$

where $N(\epsilon)$ is the state density per formula unit in the paramagnetic phase.

We now summarize how the same effects arise in LSDA. In a self-consistent calculations for a crystal the wave functions and spin densities are continuously modified, the problem being solved by iteration, and the final-converged-wave functions are eigenstates of the potential due to a nonuniform, but periodic, spin density. In LSDA the spin-polarization energy may be expressed, approximately, in terms of radial integrals

$$E^{\mathrm{LSDA}}_{\mathrm{SP}} = -\frac{1}{4}\sum_{l,l'} J_{ll'} m_l m_{l'}. \quad (7)$$

The LSDA atomic exchange integral matrices, $J_{ll'} m_l m_{l'}$, will be defined explicitly below. The energies of the conduction-electron bands in the field of the $4f$ states are then given by

$$\epsilon^{\pm}_{nk} = \epsilon_{nk} \mp \frac{1}{2} J_{4f-c}(n\vec{k}, n\vec{k})\langle \mu^z_{4f} \rangle$$
$$= \epsilon_{nk} \mp (g_J - 1) J_{4f-c}(n\vec{k}, n\vec{k})\langle J^z_{4f} \rangle. \quad (8)$$

The approximations leading to Eq. (5) are similar to those leading to Eq. (8)—the LSDA version of the rigid band splitting of Stoner theory.[38–40]

In LSDA the exchange and correlation potential is given by[41]

$$v^{\pm}_{\rm xc}(r) = A[n(r)] \left(\frac{2n^{\pm}(r)}{n(r)} \right)^{\frac{1}{3}} + B[n(r)], \quad (9)$$

where A and B are functions of the total electron density,[41] $n(r) = n^+(r) + n^-(r)$. Since the total spin-up and spin-down potentials contain $v_{\rm xc}(r)$, additively, the difference between spin-up and spin-down potentials is

$$\Delta v_{\rm xc} = v^+{}_{\rm xc}(r) - v^-{}_{\rm xc}(r). \quad (10)$$

The difference in the spin-up and spin-down potentials is a functional of the local total spin-up and spin-down densities. Since the $4f$ spin density is highly nonuniform, so is its effect upon the spin-up and spin-down potentials.

The bare exchange integrals are obtained approximately by first expanding the exchange split potential, Eq. (9), to first order in the magnetic moment density which is resolved into its partial angular momentum components, assuming that spin-up and spin-down densities do not differ, that only states close to the Fermi energy contribute to the magnetic moment, and applying first order perturbation theory by averaging with the wave function at the energy for which the splitting is required. The effective energy splitting at the Fermi energy is then

$$\Delta\epsilon(E_F) = \sum_q \sum_l \left(\frac{N_{ql}(E_F)}{N(E_F)} \sum_{l'} J_{ll'}(E_F)\mu_{ql'} + J_{4f-l}(E_F) \right), \quad (11)$$

where J_{4f-l} is given by

$$J_{4f-l}(E_F) = \frac{2}{3} \int r^2 \phi^2_{4f}(r)\phi^2_l(r, E_F) A\left[n(r)\right]/n(r) dr, \quad (12)$$

where the sum over l, l' excludes $l = 3$ and q labels the atom. The intraconduction-electron exchange integrals are

$$J_{ll'}(E_F) = \frac{2}{3} \int r^2 \phi^2_l(r, E_F)\phi^2_{l'}(r, E_F) A\left[n(r)\right]/n(r) dr. \quad (13)$$

The latter integrals are evaluated at the Fermi energy for both states l and l'. Then one obtains essentially the average splitting of the partial l bands per unit of spin moment μ'_l obtained from the potential difference, in Eq. (10) at the Fermi energy. The integrals, $J_{ll'}(E_F)$, for the rare-earth metals are calculated to be for dhcp Pr, $J_{5d5d} = 38$ mRy, $J_{5d6p} = 36$ mRy, and $J_{5d6s} = 39$ mRy; for hcp Gd, $J_{5d5d} = 39$ mRy, $J_{5d6p} = 40$ mRy, and $J_{5d6s} = 42$ mRy, and are, therefore, more or less constant across the series. The integrals $J_{4f-l}(E_F)$ are for dhcp Pr, $J_{4f-5d} = 8.6$ mRy; for hcp Gd, $J_{4f-5d} = 6.5$ mRy. Since the rare-earth contraction, which changes the $4f\,5d$ overlap, is fairly smooth the integrals may reasonably be interpolated by $J_{4f-5d} \approx 8.6 - 0.42(x-2)$ mRy, or $J_{4f-5d} \approx 117 - 5.71(x-2)$ meV where x is the number of $4f$ electrons.

Self-consistent calculations for Gd in which the $4f$ spin was varied between 0 and 7 confirmed that the $5d$ moment is an almost linear function of the $4f$ spin. The $4f\,5d$ exchange integrals actually change slightly with increasing $4f$ spin. For example, in Gd with $\mu^s_{4f} = 0, J_{4f5d} = 88$ meV whereas when $\mu^s_{4f} = 7, J_{4f5d} = 94$ meV. The $5d$ moments may be estimated from the corresponding exchange splitting of the $5d$ bands at the Fermi energy, Eq. (11), at various levels of approximation. If it is assumed that the partial $5d$ state density dominates, the ratio $\frac{N_{5d}(E_F)}{N(E_F)}$ is one half for hcp Gd. The $5d$ moment at a site is then given by

$$\mu_{5d} = \frac{J_{4f-5d}\mu^s_{4f} N_{5d}(E_F)/2}{(1 - J_{5d5d}N_{5d}(E_F)/2)}, \quad (14)$$

where J_{5d5d} is calculated to be 531 meV for Gd and $\mu^s_{4f} = 7$ is the $4f$ spin. The approximation of Eq. (14) yields results to within a few percent of the actual $5d$ moments obtained in the self-consistent spin-polarized calculations (Fig. 1). The partial $5d$ state density at the Fermi energy is calculated to be about 16 states/Ry atom in the paramagnetic state and is more or less constant across the heavy rare-earth series. The $5d$ moment for Gd is calculated to be $\mu_{5d} = 0.53\mu_B$ from Eq. (14) and to be $\mu_{5d} = 0.48\mu_B$ self-consistently in a 405 $\vec{k}$-point spin-polarized calculation. The reasons for the slightly different values are (1) above $\mu^s_{4f} = 3, N_d(E_F)$ starts to fall being only 9.2 states/Ry atom for $\mu^s_{4f} = 7$, and (2) $N_{6p}(E_F) = 5.5$ which is not negligible compared with $N_{5d}(E_F) = 16.5$. In a more complete multiband theory Eq. (14) is modified by $5d$-$5d$ and $6p$-$6p$ exchange interactions which yield an effective Stoner factor $IN_{\rm tot}(E_F)/2$, where $I = 272$ meV. With $N_{\rm tot}(E_F) = 16 + 5.5 = 21.5$ states/Ry atom, the Stoner enhancement factor is then 1.79 for the calculated values of $J_{6p6p} = 734$ meV and $J_{6p5d} = 544$ meV compared with the $5d$-$5d$ enhancement factor of 1.47 in Eq. (14).

IV. SUMMARY

In summary, the self-consistent spin-polarized calculations yielded a total conduction-electron moment for Gd of $0.65\mu_B$ from a 405 $\vec{k}$-point calculation which compares well with the measured value of $0.63\mu_B$ (Ref. 33) and suggests that LSDA gives most reasonable values for the conduction band splitting. Lindgård[30] used magnetization data to deduce the conduction-electron polarization and, from his calculated state density at the Fermi energy, evaluated the exchange interaction from the relation $\mu_{\rm cond} = \bar{S}_{4f} N(E_F) J_{4f-c}$. In this way he obtained

an effective $J_{4f-c} = 82$ meV for the series quite close to the values of J_{4f5d} given above.

We have calculated the extremal areas of the FS of Gd and Tb using LMTO-ASA method with the von Barth–Hedin exchange-correlation potential. The band structure for Gd and Tb are very similar except that in Tb the eighth band crosses the Fermi level. Thus the FS of both these metals is also very similar except that in Tb the eighth band gives rise to a small FS sheet centered along ΓK. For Gd our calculated FS areas for the bigger orbits are in agreement with those measured by MY and Schirber *et al.* To obtain the smaller FS orbits one would require shifting the Fermi level by around 5 mRy. Thus in contrast to the conclusion of Singh,[9] we believe that one does not need to explicitly include the f-d hybridization in the calculations in order to describe the small orbits. For Tb only one FS orbit has been measured and is in agreement with the calculated area. The inclusion of spin-orbit coupling changes the FS areas slightly bringing them in better agreement with experiment.

In conclusion, we have shown that a treatment of the $4f$ levels as pseudocore states gives good results for the Fermi surface and magnetic moment of Gd. However, although this has not been explicitly investigated, it is likely that the present calculational method will give a larger equilibrium volume than observed experimentally. Since the frozen core approximation as well as limitations of the local density approximation give rise to inaccuracies in the calculations of the volume, it is not presently possible to regard this discrepancy between theory and experimental as caused by the pseudocore treatment of the $4f$ electrons. Therefore, we believe that there is still no direct evidence available which shows that the $4f$ states be treated as ordinary valence states.

ACKNOWLEDGMENTS

It is a pleasure to thank D.D. Koelling and T. Gasche for valuable discussions. One of us (SA) would like to thank the Condensed Matter Theory Group, at Physics Department, Uppsala University, Sweden for their kind hospitality.

[1] M.R. Norman and D.D. Koelling, in *Handbook on the Physics and Chemistry of Rare Earths*, edited by K.A. Gschneidner Jr., L. Eyring, G.H. Lander, and G.R. Choppin (North-Holland, Amsterdam, 1993), Vol. 17, p. 1.
[2] J.O. Dimmock and A.J. Freeman, Phys. Rev. Lett. **13**, 750 (1964).
[3] S.C. Keeton and T.L. Loucks, Phys. Rev. **168**, 672 (1968).
[4] B.N. Harmon and A.J. Freeman, Phys. Rev. B **10**, 1979 (1974).
[5] B.N. Harmon, J. Phys. (Paris) **C5**, 65 (1979).
[6] J. Sticht and J. Kübler, Solid State Commun. **53**, 529 (1985).
[7] B.C.H. Krutzen and F. Springelkamp, J. Phys. C **1**, 8369 (1989).
[8] W.M. Temmerman and P.A. Sterne, J. Phys. C **2**, 5529 (1990).
[9] D.J. Singh, Phys. Rev. B **44**, 7451 (1991).
[10] B. Kim, A.B. Andrews, J.L. Erskine, K.J. Kim, and B.N. Harmon, Phys. Rev. Lett. **68**, 1931 (1992).
[11] E. Vescovo, O. Rader, T. Kachel, U. Alkemper, and C. Carbone, Phys. Rev. B **47**, 13 899 (1993).
[12] L.M. Sandratskii and J. Kübler, Europhys. Lett. **23**, 661 (1993).
[13] R.C. Young, R.G. Jordan, and D.W. Jones, Phys. Rev. Lett. **31**, 1473 (1973).
[14] J.E. Schirber, F.A. Schmidt, B.N. Harmon, and D.D. Koelling, Phys. Rev. Lett. **36**, 448 (1976).
[15] R.C. Young, R.G. Jordan, and D.W. Jones, J. Phys. F **6**, L37 (1976).
[16] P.G. Mattocks and R.C. Young, J. Phys. F **7**, 1219 (1977).
[17] S.A. Sondhelm and R.C. Young, J. Phys. F **15**, L261 (1985).
[18] C. Jackson, Phys. Rev. **178**, 949 (1969).
[19] P.G. Mattocks and R.C. Young, J. Phys. F **7**, L19 (1977).
[20] S.C. Wu, H. Li, D. Tian, Y.S. Li, F. Jona, J. Sokolov, and N.E. Christensen, Phys. Rev. B **41**, 11 911 (1990).
[21] P. Wells, P.C. Lanchester, W.D. Jones, and R.G. Jordon, J. Phys. F **4**, 1729 (1974).
[22] J. Hubbard, Proc. R. Soc. London Ser. A **276**, 238 (1963).
[23] R.A. Heaton, J.G. Harrison, and C.C. Lin, Phys. Rev. B **28**, 5992 (1983).
[24] A. Svane and O. Gunnarsson, Phys. Rev. Lett. **65**, 1148 (1990).
[25] Z. Szotek, W.M. Temmerman, and H. Winter, Phys. Rev. B **47**, 1124 (1993).
[26] H.L. Skriver, in *Systematics and Properties of the Lanthanides*, edited by S.P. Sinha (Reidel, Dordrecht, 1983), p. 213.
[27] O. Eriksson, M.S.S. Brooks, and B. Johansson, J. Less-Common Met. **158**, 207 (1990).
[28] O.K. Andersen, Phys. Rev. B **12**, 3060 (1975).
[29] H.L. Skriver, *The LMTO Method* (Springer, Berlin, 1984).
[30] P.A. Lindgård, in *Magnetism in Metals and Metallic Compounds*, edited by J.T. Lopuzanski, A. Pekalsky, and J. Przystawa (Plenum Publishing Corporation, New York, 1976), p. 203.
[31] M. Richter and H. Eschrig, Solid State Commun. **72**, 263 (1989).
[32] H.L. Skriver and I. Mertig, Phys. Rev. B **41**, 6553 (1990).
[33] L.W. Roeland, G.J. Cock, F.A. Muller, C.A. Moleman, K.A.M. McEwen, R.C. Jordan, and D.W. Jones, J. Phys. F **5**, L233 (1975).
[34] R.W. Stark (private communications).
[35] R. Ahuja, A.K. Solanki, T. Nautiyal, and S. Auluck, Pramāna J. Phys. **32**, 831 (1989).
[36] For a review, see J. Jensen and A.R. Mackintosh, *Rare Earth Magnetism, Structures and Excitations* (Oxford Science Publications, Oxford, 1991).
[37] M.A. Ruderman and C. Kittel, Phys. Rev. **96**, 99 (1954).
[38] O. Gunnarsson, J. Phys. F **6**, 587 (1976).
[39] O. Gunnarsson, Physica **91B**, 329 (1977).
[40] J.F. Janak, Phys. Rev. B **16**, 255 (1977).
[41] U. von Barth and L. Hedin, J. Phys. C **5**, 1629 (1972).